

We-01-03

## Specularity Gathers for Diffraction Imaging

I. Sturzu (Z-Terra Inc.), A.M. Popovici (Z-Terra Inc.), N. Tanushev (Z-Terra Inc.), I. Musat (Z-Terra Inc.), M.A. Pelissier (Roc Oil (Bohai) Company, formerly at Marathon Oil) & T.J. Moser\* (Moser Geophysical Services)

### SUMMARY

---

Seismic diffraction imaging is recognized as a rapidly emerging technology with great potential to reduce exploration and production risks and increase recovery, for conventional reservoirs as well as unconventional resources such as shale gas. The idea behind diffraction imaging in a pre-stack migration framework is to apply a weight factor inside the migration loops, which attenuates events that satisfy Snell's law of specular reflection, while preserving diffractive events that do not satisfy Snell's law. Conceptually, it can be paraphrased as 'switching off reflectivity during migration'. Here we present an approach, called specularity gathers, to construct the weight factor in a very efficient way, with applications on test models and the Eagle Ford shale play of South Texas. Specularity gather analysis proves to be a very useful tool to calibrate diffraction imaging, enabling the efficient construction of diffraction images and updates based on interpretation input. We expect that further development and deployment in the industry will be key in advancing diffraction imaging technology.

## Introduction

Seismic diffraction imaging is recognized as a rapidly emerging technology with great potential to reduce exploration and production risks and increase recovery, for conventional reservoirs as well as unconventional resources such as shale gas. Current research has identified a new approach to image small scale faults, pinch-outs, salt flanks, reflector unconformities, in general any small scattering objects, by using diffraction imaging as a complement to the structural images produced by reflection imaging (Khaidukov, Landa and Moser 2004, Shtivelman and Keydar, 2005, Taner, Fomel and Landa 2006, Moser and Howard 2008, Koren, Ravve and Levy, 2010, Dell and Gajewski 2011, Moser 2011).

The idea behind diffraction imaging in a pre-stack migration framework is to apply a weight factor inside the migration loops, which attenuates events that satisfy Snell's law of specular reflection, while preserving diffractive events that do not satisfy Snell's law. Conceptually, it can be paraphrased as 'switching off reflectivity during migration'. Here we present an approach to construct the weight factor in a very efficient way, with applications on test models and the Eagle Ford shale play of South Texas.

## Specularity gathers

We consider the weighted Kirchhoff migration integral

$$V(\mathbf{x}) = \int dt ds d\mathbf{r} w(\mathbf{s}, \mathbf{x}, \mathbf{r}) U(t, \mathbf{s}, \mathbf{r}) \delta(t - T(\mathbf{s}, \mathbf{x}, \mathbf{r})), \quad (1)$$

where  $U(t, \mathbf{s}, \mathbf{r})$  denotes the (second time-derivative of the) pre-stack data, depending on time  $t$  and shot/receiver position  $\mathbf{s}/\mathbf{r}$ ,  $\delta$  the Dirac delta function,  $T(\mathbf{s}, \mathbf{x}, \mathbf{r})$  the travel time from  $\mathbf{s}$  to  $\mathbf{r}$  via the subsurface image point  $\mathbf{x}$  computed by ray tracing in a given reference velocity model, and  $V(\mathbf{x})$  the resulting migrated image.

The weighting function  $w(\mathbf{s}, \mathbf{x}, \mathbf{r})$  is used to design the migration integral (1) for specific purposes. For  $w(\mathbf{s}, \mathbf{x}, \mathbf{r}) \equiv 1$  we have the standard unweighted migration (referred to as 'full-wave'). For diffraction imaging we construct the weighting function in terms of *specularity*, defined by

$$S(\mathbf{s}, \mathbf{x}, \mathbf{r}) = |\mathbf{n}^T T_{\mathbf{x}}| / \|T_{\mathbf{x}}\|, \quad (2)$$

where  $T_{\mathbf{x}}$  denotes the gradient of  $T(\mathbf{s}, \mathbf{x}, \mathbf{r})$  with respect to  $\mathbf{x}$  and  $\mathbf{n}$  the reflector unit normal, depending on  $\mathbf{x}$ . For  $\mathbf{x}$  located on a strong reflector,  $S = 1$  implies that the bisector of ray vectors from  $\mathbf{s}$  and  $\mathbf{r}$  is collinear with  $\mathbf{n}$  and hence there is pure specular reflection, for  $S < 1$  there is non-specularly scattered energy which is the objective of diffraction imaging. A convenient way to design the weighting function is to sort the migration output in *specularity gathers*:

$$V(\mathbf{x}, S) = \int dt ds d\mathbf{r} U(t, \mathbf{s}, \mathbf{r}) \delta(t - T(\mathbf{s}, \mathbf{x}, \mathbf{r})) \delta(S - |\mathbf{n}^T T_{\mathbf{x}}| / \|T_{\mathbf{x}}\|), \quad (3)$$

and obtain the final image by a weighted stack over  $S$ :  $V(\mathbf{x}) = \int_0^1 dS w(\mathbf{x}, S) V(\mathbf{x}, S)$ . This has the advantage that the weighting function is designed *after* migration and therefore constructed, and updated, very efficiently. In particular, the weighting function can be chosen spatially variable ( $w = w(\mathbf{x}, S)$ ) and adapted to the local Fresnel zone width, which is difficult to estimate *a priori* but very easily on the specularity gathers. Also feedback from interpretation can be easily included in the weighting function and hence the final appearance of the diffraction image (Figure 5). Note that the procedure of specularity gathers is very similar to sorting the migration output into common-image gathers  $V(\mathbf{x}, h)$ , where  $h$  is offset and the final image is obtained as  $V(\mathbf{x}) = \int dh \mu(\mathbf{x}, h) V(\mathbf{x}, h)$  for a given offset mute function  $\mu(\mathbf{x}, h)$ . Figure 2 offers an illustration.

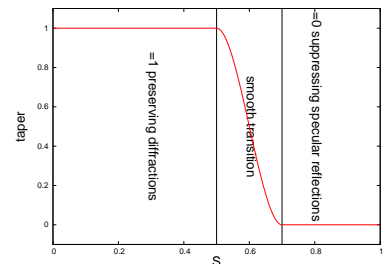


**Figure 1** Specularity weighting function  $w(S)$ .

For a correct velocity model and in the high-frequency limit, a specular reflection event appears in the specularity gathers as a focused spot on the  $S = 1$ -axis. Point diffractions appear as flat events extending over  $0 \leq S \leq 1$ . Edge diffractions in three dimensions appear as dipping events, as they obey Snell's law only along the edge, not transversely to it (Moser, 2011). Finite bandwidth reflections also appear as dipping events, as the non-specular part of reflected energy outside the Fresnel zone is not related to the shortest reflection path following Fermat's principle. In this paper, we use a piecewise cubic polynomial for the weighting function, with two cutoff specularities defining energy ranges which are suppressed/preserved and a smooth transition between them (Figure 1).

A workflow for diffraction imaging consists of: I. standard pre-stack depth migration (formula (1) with  $w \equiv 1$ ) and associated migration velocity analysis to obtain an optimally focused full-wave image  $V(\mathbf{x})$ ; II. extraction of the reflector unit normal  $\mathbf{n}$  from  $V(\mathbf{x})$  each point  $\mathbf{x}$ ; III. migrating using formula (1) with a weighting function  $w(\mathbf{s}, \mathbf{x}, \mathbf{r})$  designed to enhance diffractions/suppress reflections and obtain the diffraction image  $V^D(\mathbf{x})$ . Details and further references can be found in Moser and Howard (2008) and Moser (2011).

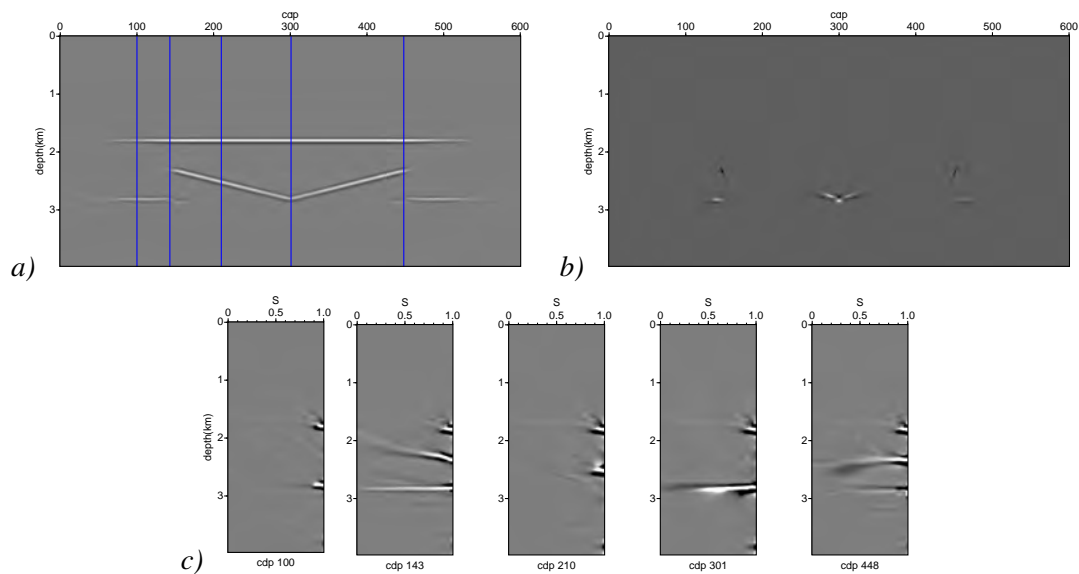


**Figure 2** a) Standard PSDM image. b) Diffraction image. c) Specularity gathers at locations indicated in Figure 2a). Energy with  $S > 0.66$  is suppressed to produce the diffraction image of Figure 2b).

### Examples - Switching off reflectivity during migration

The Kirchhoff migrations were performed using Z-Terra's prestack depth migration program ZTK, in which the diffraction imaging method was implemented through the procedure outlined above (eqs. 1-3). The first example (Figure 2) illustrates the functionality of specularity gathers on a simple diffraction ramp model. The specularity gathers of Figure 2c show focused spots at  $S = 1$  for specular reflections in the gathers at CDP 100 and 210, the other panels (143, 301, 448) show energy smeared out along flat events for  $0 \leq S \leq 1$  associated with diffractions. Suppressing energy with  $S > 0.66$  leads to the diffraction image of Figure 2.

The second example is the Mare di Cassis data set (Moser and Howard, 2008). Here setting the specularity cutoffs dependent on depth allows to optimally suppress reflectivity both in the shallow and deep sections (Figure 3).

The third example concerns production data from the Eagle Ford shale play. Here diffraction imaging has been carried out in the framework of a full 3D depth imaging process. Figure 5a shows a depth slice of the full-wave depth-migrated image, with locations for which the specularity gathers are displayed in Figure 4. Here, due to the 3D geometry, the events are considerably more complex than in the example

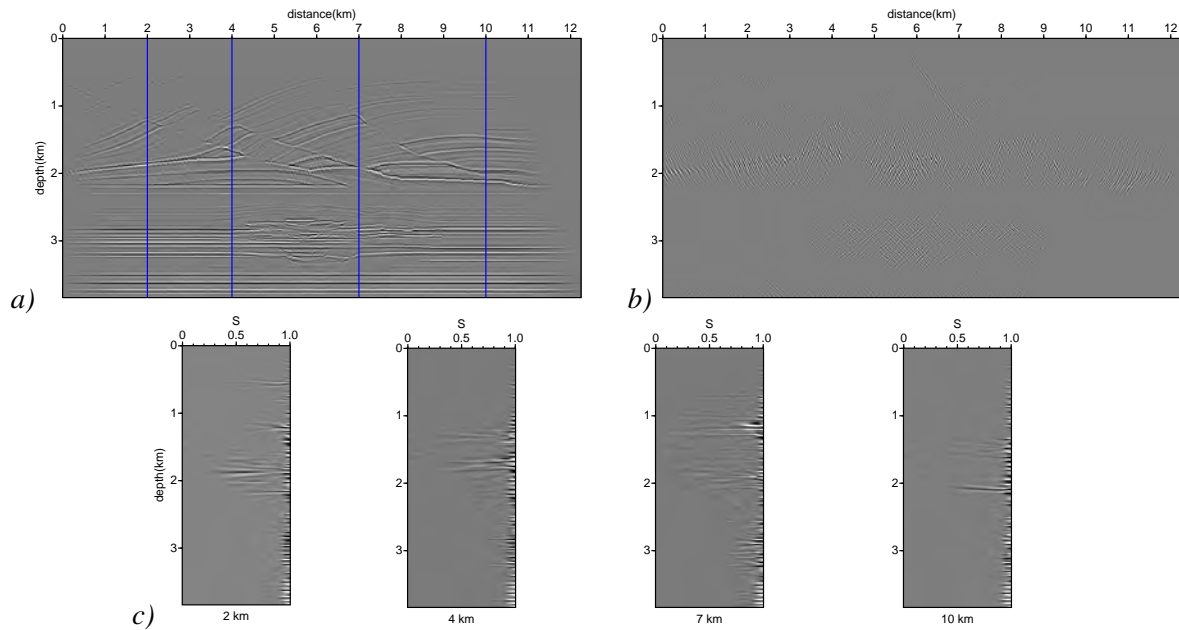


**Figure 3** Cassis. a) Standard PSDM image. b) Diffraction image (zoom for details). c) Specularity gathers at locations indicated in Figure 3a. Energy with  $S > 0.80/0.97$  (top/bottom) is suppressed to produce the diffraction image of Figure 3b.

of Figure 2. Still, suppressing reflectivity by various degrees results in diffraction images bringing up a wealth of interpretation detail (Figures 5cd, compare with the conventional coherence extraction of Figure 5b; cutouts have not been part of the survey).

## Conclusions

Specularity gather analysis proves to be a very useful tool to calibrate diffraction imaging, enabling the efficient construction of diffraction images and updates based on interpretation input. We expect that further development and deployment in the industry will be key in advancing diffraction imaging technology.

## Acknowledgements

We thank Marathon Oil and Seitel for permission to show the Eagle Ford data, and Opera (Pau) for providing the Mare di Cassis data set.

## References

- Dell, S. and Gajewski, D., 2011. Common-reflection-surface-based workflow for diffraction imaging, *Geophysics*, **76**, 187-195.
- Khaidukov V., Landa E. and Moser T.J. 2004. Diffraction imaging by focusing-defocusing: An outlook on seismic superresolution, *Geophysics*, **69**, 1478-1490.
- Koren Z., Ravve I. and Levy R. 2010. Specular-diffraction Imaging by Directional Angle Decomposition, *72nd EAGE Conference Barcelona, Extended Abstracts*.
- Moser T.J. and Howard C.B. 2008. Diffraction imaging in depth, *Geophysical Prospecting*, **56**, 627-641.
- Moser T.J., 2011. Edge and Tip Diffraction Imaging in Three Dimensions, *73rd EAGE Conference Vienna, Extended Abstracts*.
- Shtivelman V. and Keydar S. 2005. Imaging shallow subsurface inhomogeneities by 3D multipath diffraction summation, *First Break*, **23**, 39-42.
- Taner M.T., Fomel S. and Landa E. 2006. Separation and imaging of seismic diffractions using plane-wave decomposition, *76th SEG meeting, New Orleans, Expanded Abstracts*.

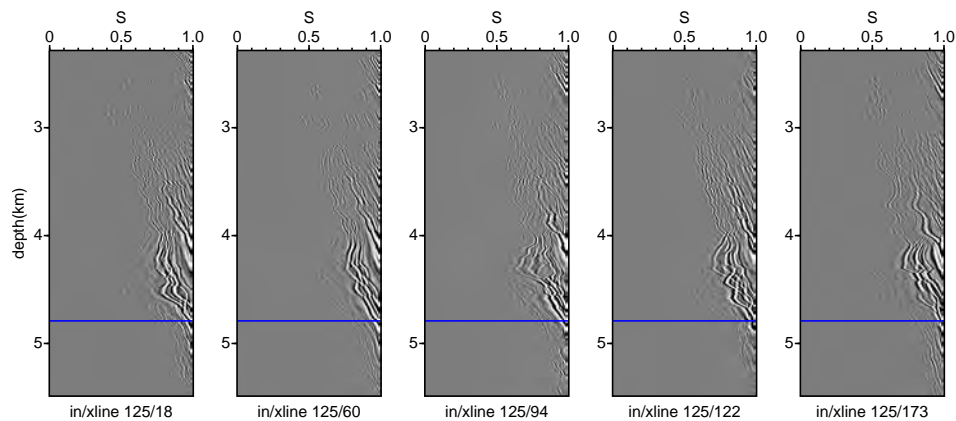


**Figure 4** Specularity gathers at in/xline locations indicated by crosses in Figure 5a.

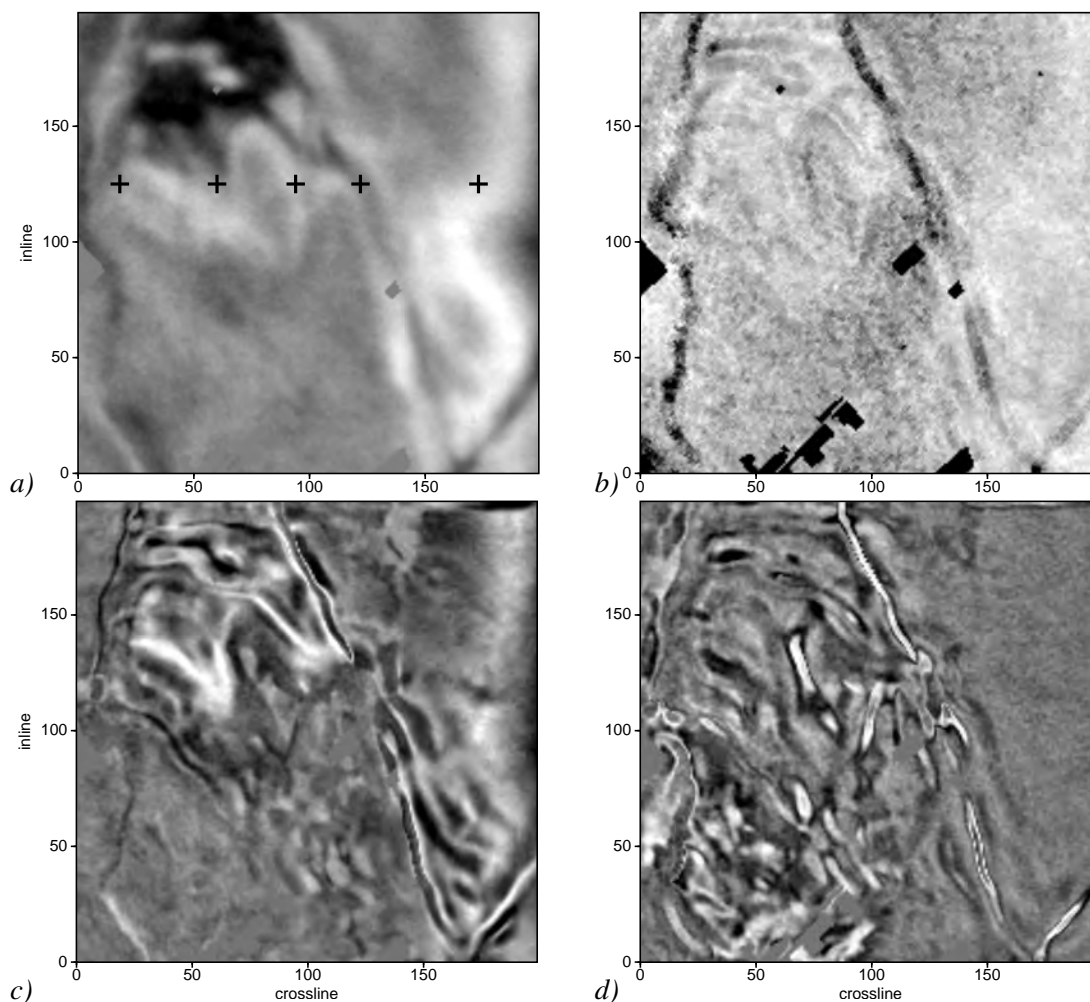


**Figure 5** Migrated images from Eagle Ford, depth slices at 4.79 km (blue lines in Figure 4). a) standard depth migration (crosses denote locations of specularity gathers in Figure 4); b) coherence slice; c,d) diffraction images with specularities above 0.99 and 0.95 suppressed, respectively. Note the increased interpretation detail in the diffraction images as (low frequency) specular reflectivity is removed.